LA-UR- 98--2930

Title: Seismic Wave Propagation Modeling

Author(s): Eric M. Jones, EES-5

Kim B. Olsen
University of California, Santa Barbara

Submitted to: DOE OFFICE OF SCIENTIFIC AND TECHNICAL INFORMATION (OSTI)

Los Alamos
NATIONAL LABORATORY

DISCLAIMER

Seismic Wave Propagation Modeling

Eric M. Jones*
Los Alamos National Laboratory

Kim B. Olsen
University of California, Santa Barbara

Abstract

This is the final report of a one-year, Laboratory Directed Research and Development (LDRD) project at the Los Alamos National Laboratory (LANL). A hybrid, finite-difference technique was developed for modeling nonlinear soil amplification from three-dimensional, finite-fault radiation patterns for earthquakes in arbitrary earth models. The method was applied to the 17 January 1994 Northridge earthquake. Particle velocities were computed on a plane at 5-km depth, immediately above the causative fault. Time-series of the strike-perpendicular, lateral velocities then were propagated vertically in a soil column typical of the San Fernando Valley. Suitable material models were adapted from a suite used to model ground motions at the U.S. Nevada Test Site. The effects of nonlinearity reduced relative spectral amplitudes by about 40 percent at frequencies above 1.5 Hz but only by 10 percent at lower frequencies. Runs made with source-depth amplitudes increased by a factor of two showed relative amplitudes above 1.5 Hz reduced by a total of 70 percent above 1.5 Hz and 20 percent at lower frequencies. Runs made with elastic-plastic material models showed similar behavior to runs made with Masing-Rule models.

Background and Research Objectives

Ground-motion modeling techniques currently in use are limited either to finite-source, linear simulations of the full two-dimensional (2-D) or three-dimensional (3-D) wave field in arbitrary earth models (e.g. finite-difference methods) or strongly simplified nonlinear simulation in layered earth models [e.g., plane, vertically incident, horizontal shear waves (SH)in the widely-used SHAKE code]. However, in the near-field of an earthquake, the source is typically not described accurately as a plane, vertically incident SH wave. Moreover, lateral variations of the elastic and inelastic material properties of the near-surface layers can be significant. In such cases, existing simulation methods may not be sufficient to accurately model ground motions. The present study is a step toward a full 3-D nonlinear modeling capability that combines the advantages of existing linear and nonlinear finite-difference ground-motion-modeling codes.

---

*Principal Investigator, e-mail: honais@lanl.gov

Importance to LANL's Science and Technology Base and National R&D Needs

Ground motion modeling has a long history at Los Alamos, beginning with the underground nuclear test program and studies of weapons effects, continuing with verification research for the Comprehensive Test Ban Treaty, and now broadening into research into earthquake hazards for major urban centers. This project takes advantage of Los Alamos strengths in numerical methods and material response and couples those with UC-Santa Barbara's world-class earthquake modeling capabilities. New capabilities to model nonlinear motions in the earthquake context will have direct applications to the Los Alamos Urban Security project and to developing collaborations with the Southern California Earthquake Center and others and will also enhance Los Alamos capabilities in weapons effects and treaty monitoring.

Scientific Approach and Accomplishments

Modeling Technique

Our modeling technique proceeds in two steps. The first is a linear, kinematic computation of the 3-D, finite-fault radiation pattern to a datum below the region affected by nonlinearity. This is followed by a nonlinear wave propagation to the ground surface using the velocity histories computed at 5-km depth in the first step.

The linear modeling is carried out with a 4th-order, staggered-grid, finite-difference method that is proven to be efficient and flexible for large-scale wave propagation simulations [9]. The linear code allows a variety of kinematic sources [8] and includes absorbing boundary conditions at the edges of the grid [5] as well as a sponge zone to minimize artificial reflections [4].

The nonlinear modeling is carried out with the Los Alamos stress-wave modeling code SMC123 [6]. SMC123 can be run in one, two, or three dimensions and utilizes elastic-plastic material constitutive rules. These are very similar to the ones used by App and Brunish [1] to produce accurate simulations of ground motions observed at the surface and in deep satellite holes in the vicinity of underground nuclear tests at the Nevada Test Site. In addition, elastic-plastic models of material behavior can be replaced with a Masing Rule description (e.g. [3]).

3-D Computation of Northridge Motions at Depth

We used the 17 January 1994 Northridge earthquake to test our hybrid finite-difference approach. The simulated earthquake rupture propagates radially outward from the hypocenter with a rupture velocity of 3 km/s and is described by the combined, variable

slip-and-rake model of Wald et al [10]. The linear, 3-D finite-fault wave field is simulated to a datum at a depth 5 km below the San Fernando Valley within an area of 17 km by 19 km immediately above the fault plane (see Figure 1). Peak particle velocities on the 5-km-deep datum are shown in Figure 2 and the maximum values are listed in Table 1. The largest velocities occur over the northern portion of the fault due to source directivity, in agreement with the low-frequency results of Olsen and Archuleta [8]. Velocity histories were computed directly below the Van Norman Complex (Figure 1), where some of the strongest motions produced by the earthquake were recorded. These are shown in Figure 3. The largest lateral velocities are about 0.3 m/s.

Linear Near-Surface Stress Levels

To obtain an estimate of the elastic strain levels expected above the datum in the San Fernando Valley, we propagated simulated P-SV waves along a strike-perpendicular profile (shown in Figure 1) into a plane-layered soil distribution using a 2-D visco-elastic finite-difference method. The distribution with depth of the densities and the P-wave and S-wave velocities are shown in Figure 4 and were taken from the geology-based, 3-D Los Angeles basin model of Magistrale et al [7]. The specific values represent a vertical column at a site within the Van Norman Complex. The estimated peak stresses are shown in Figure 5 and exceed 10 bars in the layers shallower than 300-m depth. With relatively little information available on in-situ rock strength in the region, it is uncertain whether failure of the rocks or other nonlinear behaviors occurs at these stress levels. However, in comparing the peak elastic-stress levels from the San Fernando Valley simulation with those for near-surface alluvium at the U.S. Nevada Test Site (where nonlinear behavior at similar stress levels is well documented [1]), we infer that sites in the San Fernando Valley may have experienced nonlinear ground motions during the Northridge earthquake. The present study addresses that possibility.

Nonlinear Effects

Examination of nonlinear effects was done using SMC123 by simulating the vertical propagation of planar SH-waves in a 1-D soil column. The distribution of densities and velocities shown in Figure 4 was approximated by dividing the soil column into 5 homogeneous layers. The bottom depth, density, and velocities of each layer are listed in Table 2. In addition, we adopted plausible values of the shear moduli and shear strengths from Nevada Test Site materials with similar densities and velocities [1]. These and other properties were used in two different types of simulations. One set of simulations used elastic-plastic material models and a second set used the Masing Rule.

As a first step in the examination of nonlinear effects in the soil column, we propagated planar, gaussian SH waves up the soil column. Four runs were made using the elastic-plastic material models and these were then repeated using the Masing Rule. In each run, the gaussian half width was 0.2 seconds and the peak amplitude at 5-km depth was 0.3, 0.6, 0.9, or 1.2 m/s. The 0.3-m/s case was chosen to have a peak amplitude similar to that seen at 5-km depth in the 3-D linear simulation. The simulated surface ground motions are shown in Figure 6 where the amplitudes of the 0.6, 0.9, and 1.2 m/s cases have been divided by factors of 2, 3, and 4, respectively. Using this normalization, the curves would be coincident in the absence of nonlinear effects. In both the elastic-plastic series and the Masing series, the peak surface velocities for the 0.3 m/s cases are about 4 times the peak at 5-km depth and, for higher source amplitudes, amplification by the soil column is reduced by the effects of nonlinearity. In the elastic-plastic series, the amplification for the 1.2 m/s case is only about a factor of 2 while the 1.2-m/s Masing Rule case shows an amplification of slightly less than 3. As expected, use of the Masing Rule introduces a time delay in the peaks due to a reduction in the effective shear modulus [3], while use of the elastic-plastic models introduces little or no time delay. Figure 7 shows normalized velocity spectra for the gaussian cases where, as expected, the effects of nonlinearity are most pronounced at higher frequencies.

The next step in evaluating the effects of nonlinearity was to vertically propagate plane SH waves with the velocity histories derived from the strike-perpendicular motions in Figure 3. Three runs were made with the elastic-plastic material models. One was a linear case that used the strike-perpendicular velocity amplitudes divided by a factor of 1000. A second run used the velocity history without modification, and a third was done with the amplitudes multiplied by a factor of two. These three runs were then repeated using the Masing Rule. Figure 8 shows normalized velocity spectra where spectral amplitudes for the unmodified and factor-of-two cases have been divided by factors of 1000 and 2000, respectively, so that, in the absence of nonlinearity, the curves would coincide with the linear case. As was seen in the cases with gaussian sources, amplitude reductions due to nonlinearity are more pronounced for the elastic-plastic model but, in general, the results for the elastic-plastic model and for the Masing Rule are similar. For frequencies greater than 1.5 Hz, amplitudes for the unmodified velocity history (dashed curves) are reduced by about a factor of two from the linear case while, at lower frequencies, amplitude reductions are about 10 percent.

We conclude that, to the extent that the material models used in the simulations represent materials actually present in the San Fernando Valley, ground motions produced by the Northridge earthquake were subject to the effects of nonlinearity. One effect that

was not prominent in the simulations was a shift of the dominant frequencies to lower values as would be produced by a reduction in the effective shear modulus [3]. This unexpected result is discussed in the following paragraphs.

Masing Rule material models are based on the assumption that if stress τ is related to strain γ during the initial loading by the stress-strain relation

$$\tau = f(\gamma) \qquad (1)$$

then, during subsequent unloading, the stress is given by

$$(\tau - \tau_r) / 2 = f([\gamma - \gamma_r) / 2] \qquad (2)$$

where τ_r and γ_r are the stress and strain at the most recent strain reversal. Generally, stress-strain relations are anti-symmetric, with $f(-\gamma) = - f(\gamma)$ and converge on a limiting stress at large strains.

The left portion of Figure 9 shows a stress-strain path for a strain history that is a pure , 1-Hz sine wave. The curve starts at zero strain and zero stress and follows the initial loading path upward to the right. The slope of the initial portion of the loading curve is proportional to the shear modulus. The first strain reversal occurs at 0.25 seconds and subsequent motions trace out a closed hysteretic loop. Note that the major axis of the loop is inclined to the initial segment of the loading path. The slope of the major axis is proportional to the effective shear strain and, in most cases, is less than the initial modulus. For a single-frequency source, the modulus reduction produces a time delay in a velocity history or a frequency reduction in a velocity spectrum. The larger the amplitude of the single-frequency source, the larger the area of the hysteresis loop and the lower the effective shear modulus.

The right portion of Figure 9 shows a case of a dual-frequency source in which a 4.3 Hz sine wave has been added to the 1-Hz sine wave but with an amplitude only 0.3 times as large. The amplitude of the 4.3-Hz component is large enough to produce frequent strain reversals and the resulting hysteresis loops necessarily are of smaller area and have effective shear moduli closer to the initial value. The net result would be significant damping and a slight frequency shift of the 4.3-Hz component but minimal

damping and frequency shift of the 1-Hz component. We believe that behavior of this type explains the Masing series results shown in Figure 8.

Future Work

Further work on ground motion modeling in the Los Angeles Basin and on the effects of nonlinearity will be carried out as part of another LDRD project (Urban Security). The study of nonlinear effects with SMC123 will be extended to two dimensions. Because elastic-plastic and Masing Rule material models gave similar results, a Masing Rule capability, being the simpler approach, will be incorporated in the 4th-order, elastic-wave code so that direct comparisons can be made with data from the Van Norman Complex [2]. The seismic velocities, densities, and nonlinear parameters used in the models will be refined based on the result of the project Resolution of Site Response Issues from the Northridge Earthquake (ROSRINE).

Publication

Jones, E.M. and Olsen, K.B., "Three-dimensional finite-difference modeling of nonlinear ground motion", Proceedings of the Northridge Earthquake Research Conference, August 20-22, 1997 (in press).

References

[1] App, F.N. and Brunish, W.B., "Stress wave calculations for four selected underground nuclear tests: Merlin, Hearts, Presidio, and Misty Echo," Los Alamos National Laboratory Document EES-NTC-91-03 (1991).

[2] Bardet, J.P. and Davis, C., "Engineering observations on ground motion at the Van Norman Complex after the 1994 Northridge earthquake," *Bull. Seis. Soc. Am.* **86**, S333-S349 (1996).

[3] Beresnev, I. and Wen, K.L., "Nonlinear soil response - a reality?," *Bull. Seis. Soc. Am.* **86,** 1964-1978 (1996).

[4] Cerjan, C, Kosloff, D., Kosloff, R., and Reshef, M., "A non-reflecting boundary condition for discrete acoustic and elastic wave equations," *Geophysics* **50**, 705-708 (1985).

[5] Clayton, R. and Enquist, B., "Absorbing boundary conditions for acoustic and elastic wave equations," *Bull. Seis. Soc. Am.* **71**, 1529-1540 (1977).

[6] Dey, T.N. and Kamm, J.R., "User's Guide to SMC-2D v3.1," Los Alamos National Laboratory document.

[7] Magistrale, H., McLaughlin, K., and Day, S., "A geology-based 3-D velocity model of the Los Angeles Basin sediments," *Bull. Seis. Soc. Am.* **86**, 1161-1166 (1996).

[8] Olsen, K.B. and Archuleta, R.J., "3-D simulation of earthquakes on the Los Angeles fault system," *Bull. Seis. Soc. Am.* **86**, 575-596 (1996).

[9] Olsen, K.B., Archuleta, R.J., and Matarese, J.R., "Three-dimensional simulation of a magnitude 7.75 earthquake on the San Andreas fault," *Science* **270**, 1628-1632 (1995).

[10] Wald, D.J., Heaton, T.H., and Hudnut, K.W., "The slip history of the 1994 Northridge, California, earthquake determined from strong-motion, teleseismic, GPS, and leveling data," *Bull. Seis. Soc. Am.* **86**, S49-S70 (1996).

Table 1

Maximum Peak Velocities at 5-KM Depth

Strike Parallel Component (m/s)	0.71
Strike Perpendicular Component (m/s)	1.45
Vertical Component (m/s)	1.52
Total Vector (m/s)	1.80

Table 2
Material Parameters for Assumed Soil Column

Material	1	2	3	4	5
Layer Bottom (km)	0.03	0.72	1.35	3.60	–
Density (g/cm^3)	1.7	1.7	2.0	2.4	2.7
P-Wave Speed (m/s)	268	535	1069	2140	3208
Shear Modulus (GPa)	0.12	0.49	2.3	11	28
Shear Strength (Gpa)	0.020	0.033	0.020	0.090	0.090

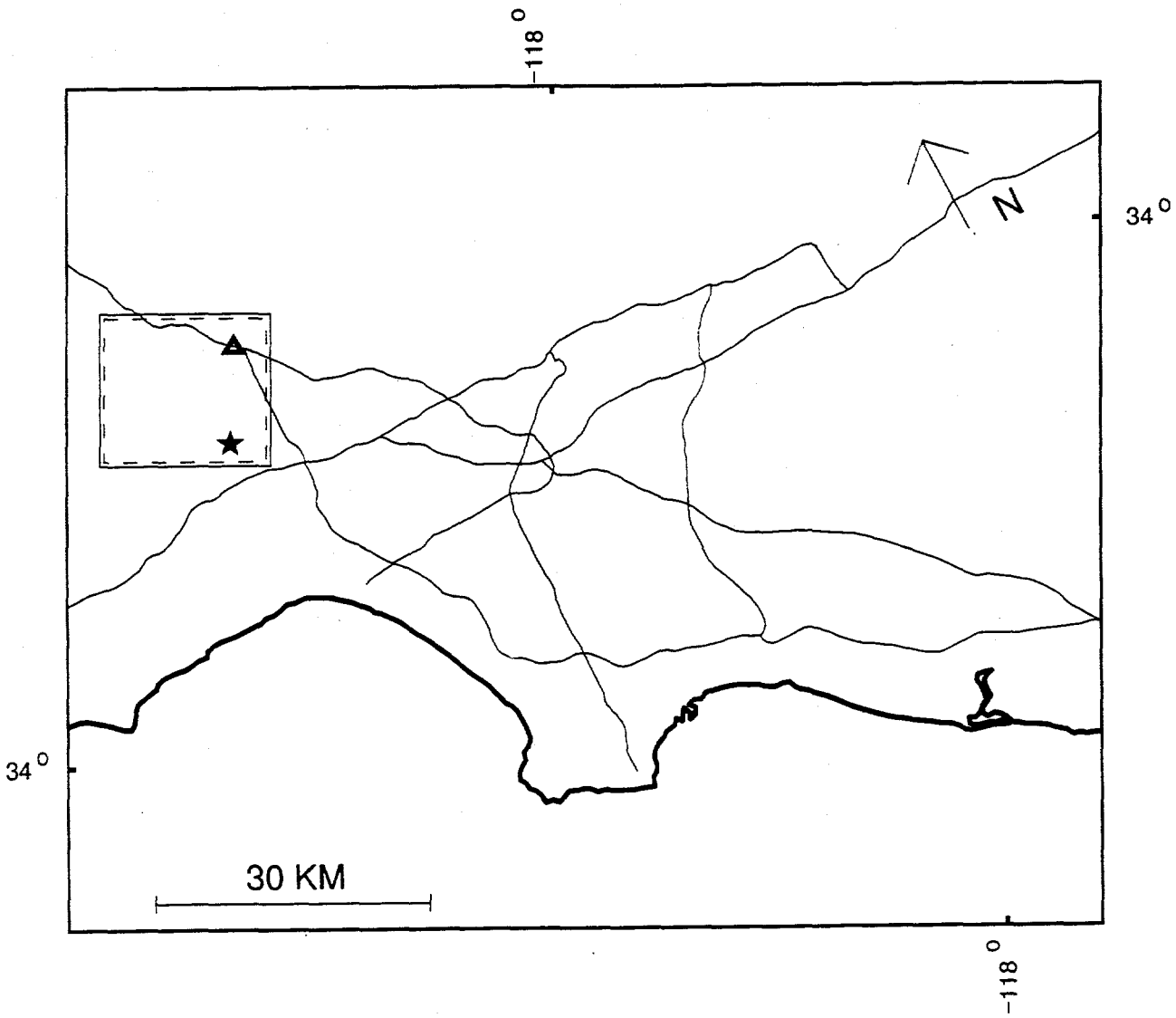

Figure 1. Map of the Los Angeles area. The dashed rectangle shows the projection of the Oak Ridge fault that ruptured during the Northridge earthquake and the solid rectangle shows the area where velocity histories have been computed at 5-km depth. The star shows the surface location over the hypocenter and the triangle shows the Van Norman Complex where some of the largest ground motions were recorded. The thin lines depict major freeways in the area.

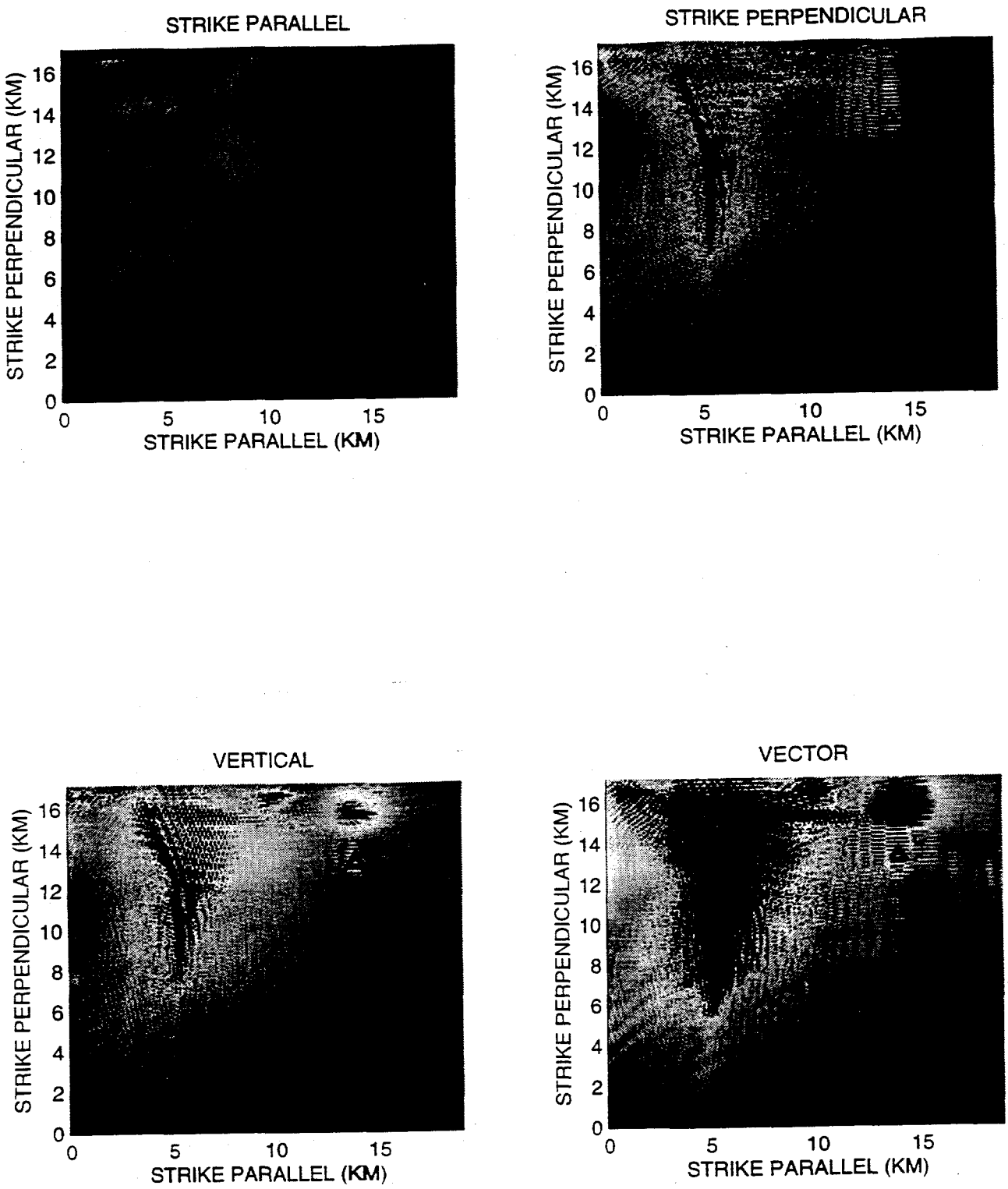

Figure 2. 0-7 Hz peak velocities for the Northridge earthquake calculated on a datum 5-km below the San Fernando Valley in the area shown in Figure 1. The maps are plotted on a common gray scale to ease inter-comparisons. The maximum value for each component is listed in Table 1. The strike parallel component is positive in the N122E direction while the strike perpendicular component is positive in the N32E direction. Note that the strike-perpendicular and vertical components are much larger than the strike parallel component because of a predominantly thrust rupture mechanism. Similarly, the northern (top left) experienced the largest motions because of directivity effects.

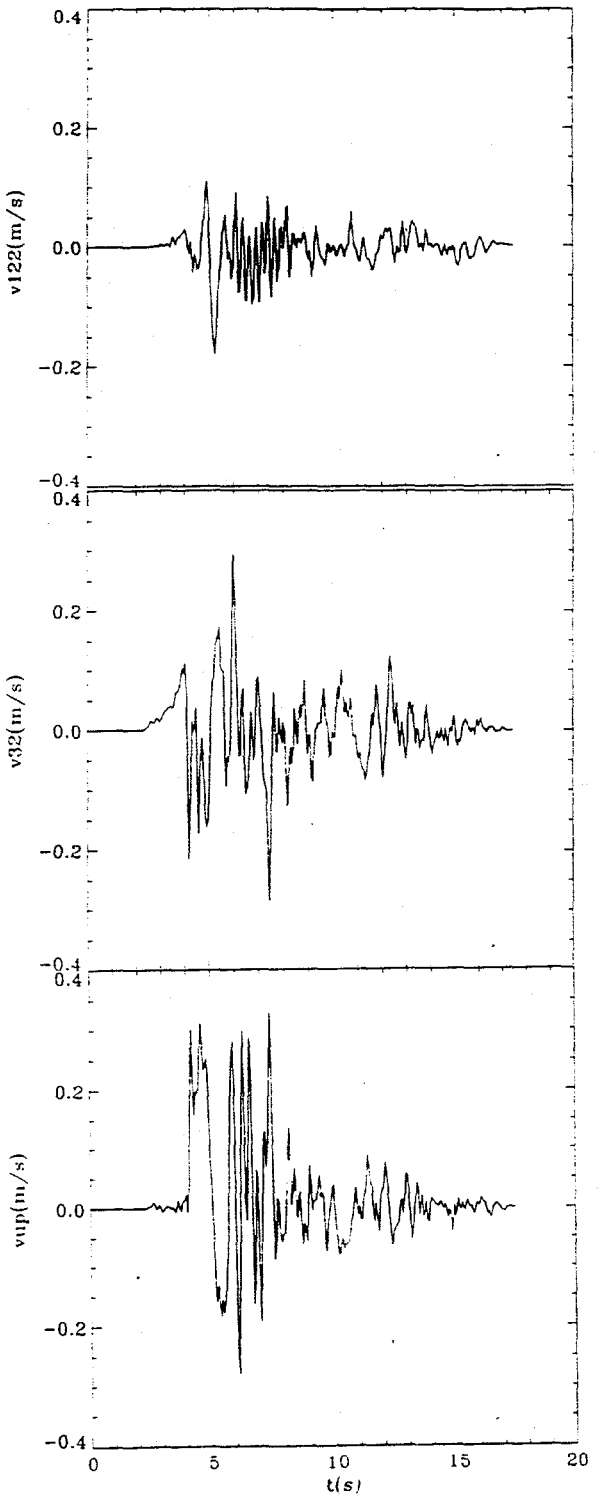

Figure 3. Simulated 0-7 Hz velocity histories at 5-km depth below the Van Norman Complex.

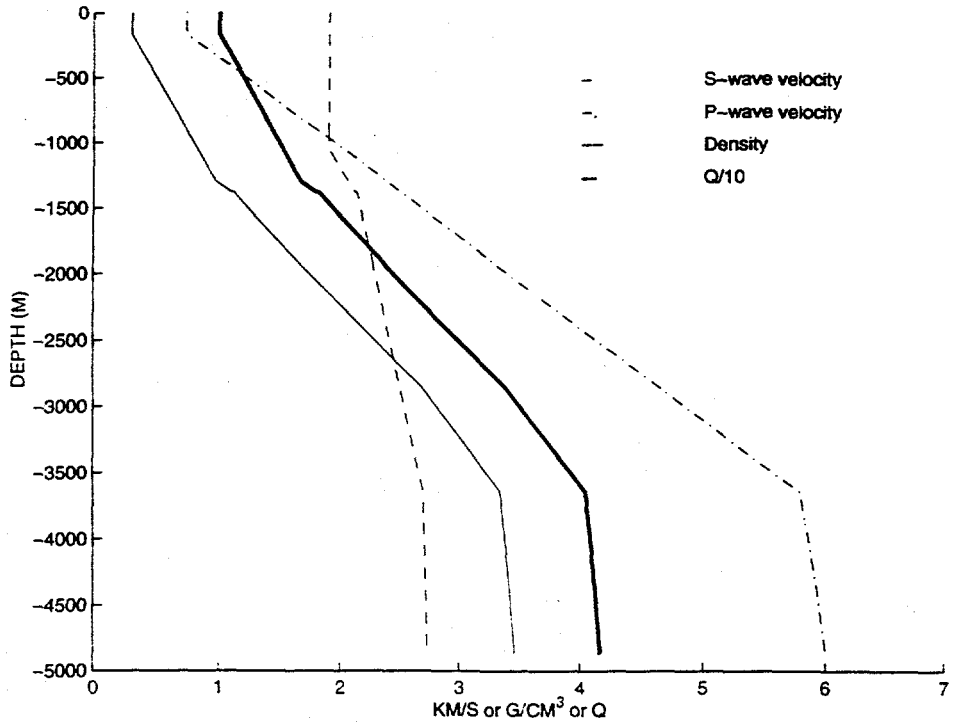

Figure 4. Elastic parameters used to estimate elastic stresses at the Van Norman Complex. The velocities and densities were taken from [7].

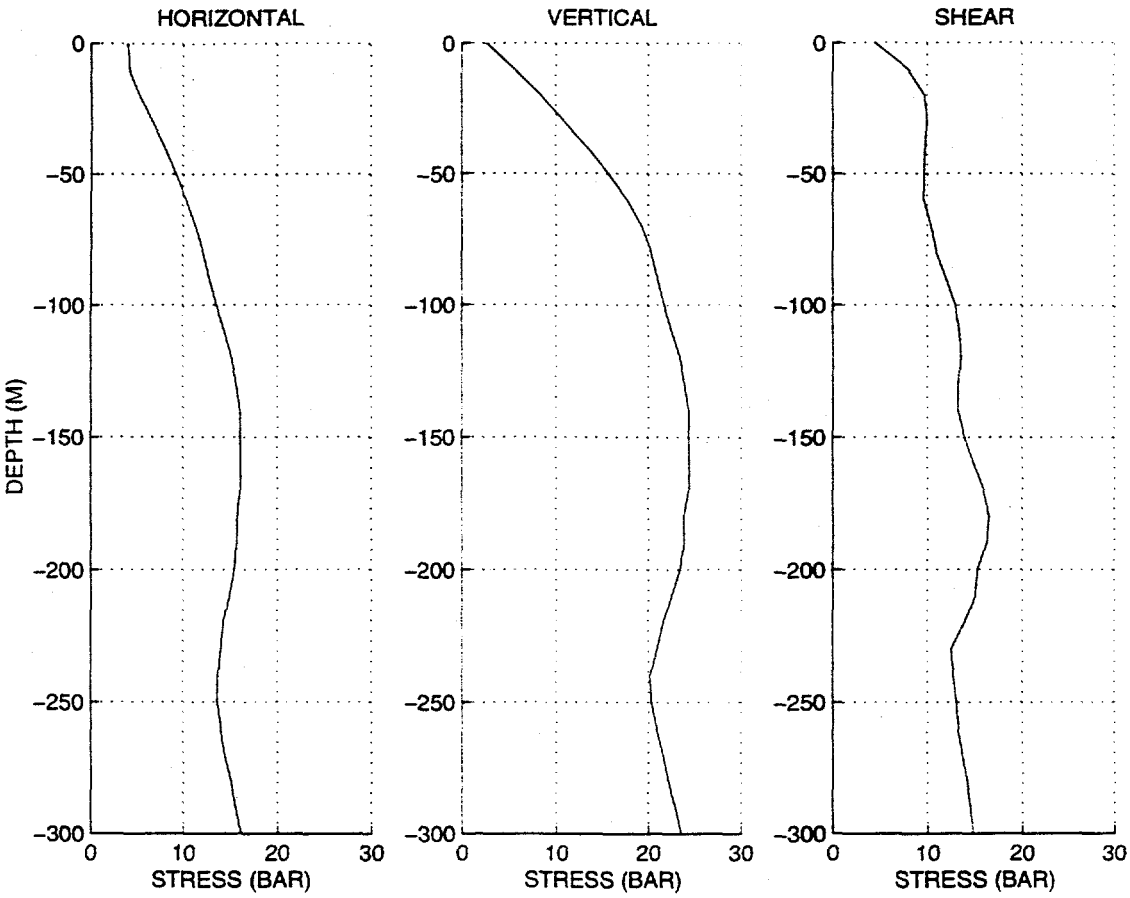

Figure 5. Estimated peak normal stresses and peak shear stress in the upper 300 m at the Van Norman Complex computed using a 2-D visco-elastic finite-difference method and the velocity histories shown in Figure 3. The estimated peak stresses exceed 10 bars, which is an approximate threshold for the initiation of nonlinear behavior in near-surface alluvium at the U.S. Nevada Test Site [1].

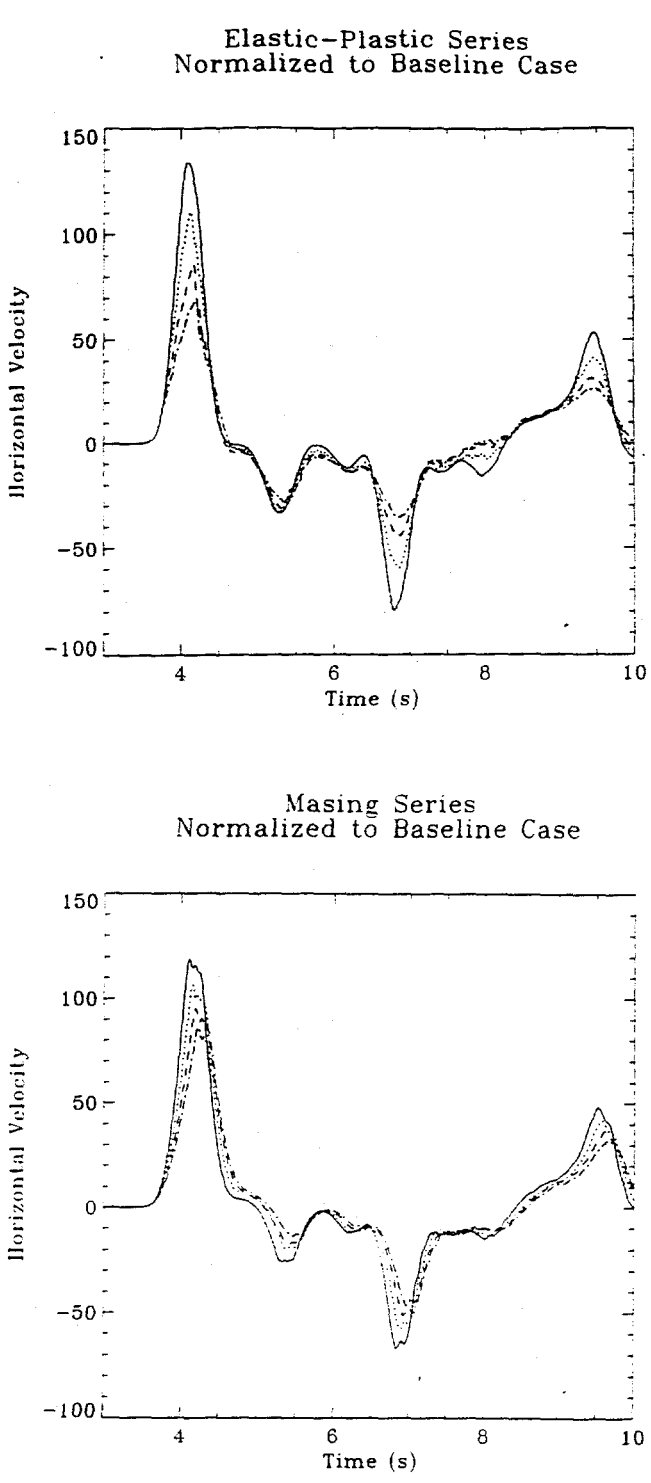

Figure 6. Horizontal velocity histories computed at the surface for cases with vertically propagated, plane-gaussian SH wave sources. The curves were computed with either elastic-plastic material models (top) or Masing Rule models (bottom). The gaussian sources all had half-widths of 0.2 sec and peak amplitudes at the 5-km source depth of 0.3 m/s (solid), 0.6 m/s (dotted), 0.9 m/s (dashed), or 1.2 m/s (dot-dash). The surface velocity curves were then divided by factors of 1.0, 2.0, 3.0, and 4.0, respectively, so that, in the absence of nonlinear effects, the curves in each plot would be coincident.

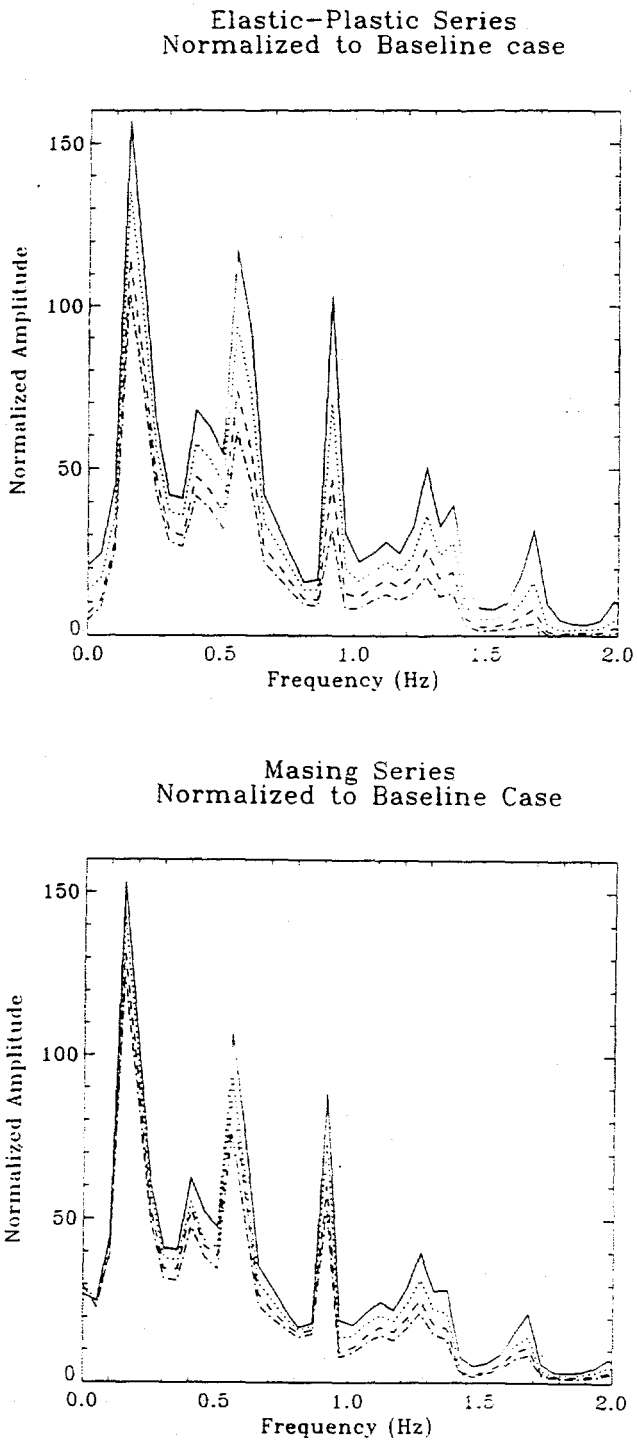

Figure 7. Horizontal velocity spectra for the same cases shown in Figure 6. These curves were normalized in the manner described in the Figure 6 caption.

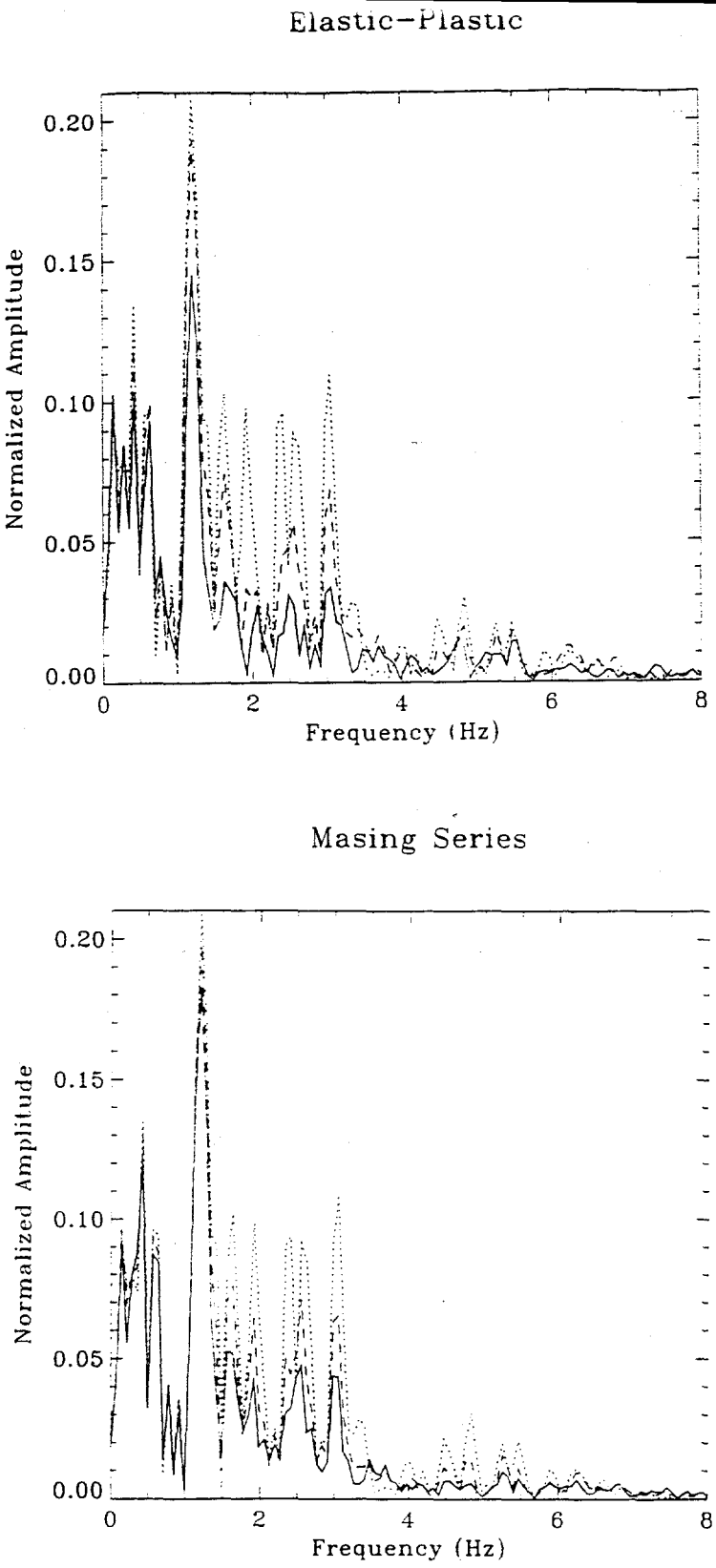

Figure 8. Horizontal velocity spectra for cases using elastic-plastic models (top) or Masing Rule models (bottom) and plane SH wave sources with time histories proportional to the strike-perpendicular history that is shown in the middle panel of Figure 3. The three cases used the strike-perpendicular velocity history multiplied by factors of 0.001 (dotted), 1.0 (dashed), or 2.0 (solid) and the surface velocity curves were then normalized by dividing by factors of 1.0, 1000, or 2000, respectively.

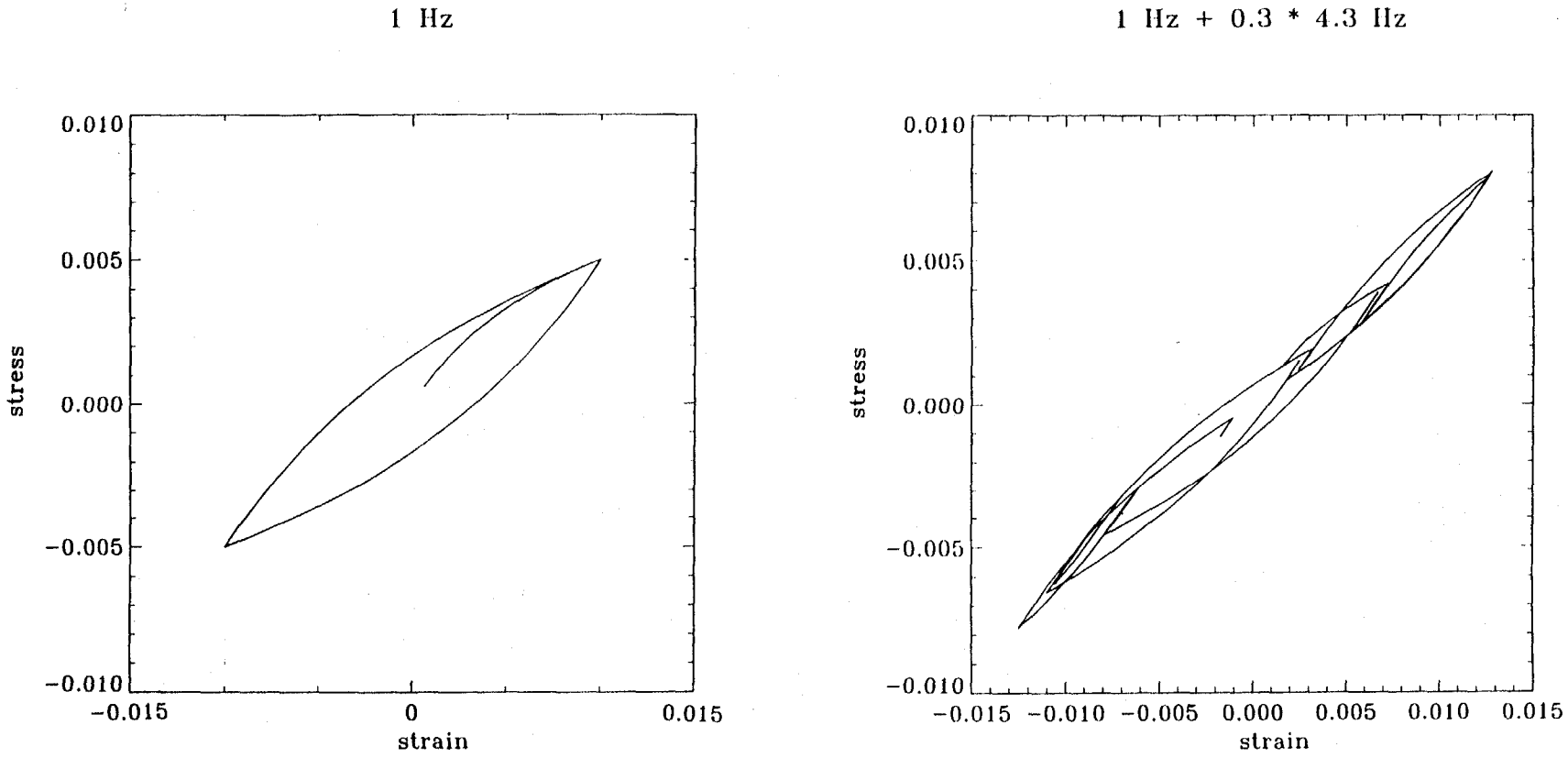

Figure 9. Simulated Masing Rule stress-strain paths for a 1-Hz sine wave (left) and a combination of a 1-Hz sine wave and a 4.3-Hz sine wave (right) where, in the latter case, the 4.3-Hz component has an amplitude 0.3 times that of the 1-Hz component.